JVSTB Journal of Vacuum Science & Technology B

Minimization of line edge roughness and critical dimension error in electron-beam lithography

Xinyu Zhao, Soo-Young Lee, Jin Choi, Sang-Hee Lee, In-Kyun Shin, and Chan-Uk Jeon

Citation: Journal of Vacuum Science & Technology B **32**, 06F505 (2014); doi: 10.1116/1.4899238
View online: http://dx.doi.org/10.1116/1.4899238
View Table of Contents: http://scitation.aip.org/content/avs/journal/jvstb/32/6?ver=pdfcov
Published by the AVS: Science & Technology of Materials, Interfaces, and Processing

Articles you may be interested in

Erratum: "Proximity exposure effect analysis using the phenomenon of resist debris formation in electron beam lithography" [J. Vac. Sci. Technol. B 20, 710 (2002)]
J. Vac. Sci. Technol. B **20**, 1578 (2002); 10.1116/1.1497167

Proximity exposure effect analysis using the phenomenon of resist debris formation in electron beam lithography
J. Vac. Sci. Technol. B **20**, 710 (2002); 10.1116/1.1463725

Comparative study of resolution limiting factors in electron beam lithography using the edge roughness evaluation method
J. Vac. Sci. Technol. B **19**, 2488 (2001); 10.1116/1.1410087

Contrast limitations in electron-beam lithography
J. Vac. Sci. Technol. B **17**, 2945 (1999); 10.1116/1.590930

Low voltage electron beam lithography in PMMA
J. Vac. Sci. Technol. B **17**, 1366 (1999); 10.1116/1.590762

Redistribution subject to AVS license or copyright; see http://scitation.aip.org/termsconditions. Download to IP: 131.204.21.179 On: Tue, 11 Nov 2014 14:57:14

CrossMark
click for updates

Minimization of line edge roughness and critical dimension error in electron-beam lithography

Xinyu Zhao and Soo-Young Lee[a]
Department of Electrical and Computer Engineering, Auburn University, Auburn, Alabama 36849

Jin Choi, Sang-Hee Lee, In-Kyun Shin, and Chan-Uk Jeon
Samsung Electronics Co., Ltd., Mask Development Team, Hwasung, Gyeonggi-Do, South Korea

(Received 6 July 2014; accepted 10 October 2014; published 28 October 2014)

As the minimum feature size continues to decrease, the line edge roughness (LER) has become a critical issue to be addressed. The LER is caused by a number of stochastically fluctuating effects involved in the fabrication process using electron-beam lithography. Since the LER does not scale with the feature size, it can significantly limit the minimum feature size and the maximum circuit density that can be achieved in a pattern of nanoscale features. Many of the efforts to decrease the LER in the past took an empirical or trial-and-error approach. In this study, a computational approach is taken in developing effective methods to minimize the LER, taking the critical dimension (CD) error due to the proximity effect also into account. Since the LER and the CD error vary with the resist-depth dimension, a 3D model is employed instead of a 2D model used in most of the previous work. The simulation results show that the proposed methods have potential to provide a practical and effective way to minimize the LER. © *2014 American Vacuum Society*.
[http://dx.doi.org/10.1116/1.4899238]

I. INTRODUCTION

One of the frequently used techniques in nanofabrication is electron beam lithography (EBL). The EBL is capable of writing patterns in the resist with extremely high resolution and has been used in fabrication of photomasks, low-volume production of semiconductor devices, experimental circuit patterns, etc.[1–4] A well-known issue in the EBL is the proximity effect due to electron scattering, which causes deviation from the target dimensions of a feature in the written pattern. Many proximity effect correction (PEC) schemes have been devised, i.e., dose modulation, pattern biasing, GHOST, etc.,[5–8] to improve critical dimension (CD) accuracy. Another issue, which could be ignored for large features in the past, is the variation or roughness of feature boundaries. As the minimum feature size routinely goes well below 50 nm, the relative roughness compared to the feature size has become significant and therefore cannot be ignored anymore. One of the widely used measures of the roughness is line edge roughness (LER). The LER is caused by a number of stochastically fluctuating effects such as shot noise, distributions of chemical species in the resist such as photoacid generator (PAG), resist development process, etc. Since the LER does not scale with the feature size, it can significantly limit the minimum feature size and maximum circuit density that can be realized. In fact, when the feature size is reduced close to the resolution limit, the LER may even increase due to the increased fluctuation and decreased contrast of exposure. Therefore, it is necessary to minimize the LER in order to be able to continue enhancing the feature resolution and pattern density that can be achieved by the EBL. Many of the efforts to reduce the LER in the past took an empirical or trial-and-error approach. However, a systematic approach was taken in some of the more recent efforts such as the multipass grayscale exposure techniques[9,10] and the resist reflow process.[11] For example, in the multipass grayscale exposure technique, each feature is exposed n times with roughly $1/n$ of the nominal dose in each pass. It has been shown that these techniques can reduce the LER and thereby enhance the device performance.

In our previous study, the dependency of LER on various lithographic parameters was analyzed through extensive simulation. In the simulation results, the following behaviors of the LER were observed. (1) The LER is substantially larger at a lower layer of resist. (2) The LER decreases as the dose increases (within a reasonable range of dose). (3) As the edge location is moved from the inside of the feature to the outside, the LER decreases. (4) The LER is smaller for a smaller exposing interval. (5) For different types of resist, though the LER level may be different, the similar behaviors of LER are exhibited.

In this study, a computational approach to minimizing the LER is taken. Two methods developed for the LER minimization are based on the behaviors of the LER observed in the previous study and also utilize the fact that the dose given to a different region affects the spatial distribution of exposure (energy deposited in the resist) differently. In one method, only the shape of a feature is adjusted with a uniform dose to minimize the LER, taking the CD error also into account. In the other method, the shape of a feature is adjusted, and the spatial distribution of dose within the feature is also controlled. In most of the previous work on the LER, a two-dimensional (2D) model was used, ignoring any variation along the resist depth dimension. However, as shown in our previous study, the LER and the CD error exhibit different behaviors at different resist layers. Therefore, a 3D model of the substrate system is employed in this study to develop

[a]Electronic mail: leesooy@eng.auburn.edu

Redistribution subject to AVS license or copyright; see http://scitation.aip.org/termsconditions. Download to IP: 131.204.21.179 On: Tue, 11 Nov 2014 14:57:14

LER minimization methods that can obtain realistic results. In this paper, the two methods are described in detail, and their effectiveness is analyzed with two different types of resists, i.e., poly(methylmethacrylate) (PMMA) and a chemically amplified resist (CAR) poly(4-hydroxystyrene) (PHS).

The rest of the paper is organized as follows. The simulation model is described in Sec. II. The two methods for LER minimization are described in Sec. III. Simulation results are discussed in Sec. IV, followed by a summary in Sec. V.

II. SIMULATION MODEL

In this section, the issues related to the simulation of e-beam lithographic process leading to the LER are described. They are stochastic exposure, conversion of exposure to developing rate, simulation of resist development, and evaluation of the LER.

A. Stochastic exposure

The stochastic exposure distribution $e(x, y, z)$ may be obtained by employing the Monte Carlo simulation at each point exposed by the e-beam, which is equivalent to generating an instance of stochastic point spread function (PSF) (see Fig. 1) for each point exposed. Note that a PSF describes how the electron energy is deposited throughout the resist (i.e., exposure distribution) when a single point is exposed. This approach may lead to more realistic exposure distribution (derived through convolution between the stochastic PSF and dose distribution). However, its computational complexity is too high to be practical for most patterns of realistic size. Hence, a new method to greatly reduce the number of stochastic PSF (instances) to be generated, referred to as the simplified Monte Carlo simulation (SMC) method, was recently developed.[12] It generates only a small number of stochastic PSF (instances) and selects a PSF instance randomly for each point exposed for calculation of the exposure distribution. Note that we are mainly interested in certain measures of the exposure fluctuation, not the exact distribution of the exposure itself. Through the simulation, it was shown that the SMC method is able to generate exposure distributions statistically equivalent to those by the direct Monte Carlo method. Therefore, in this study, the SMC method is employed without compromising the accuracy of modeling the LER.

A typical substrate system is shown in Fig. 2 where the X-Y plane corresponds to the resist surface and the Z-axis is along the resist depth dimension. The set of PSFs (instances) generated is denoted by $\tilde{S} = \{\mathrm{psf}_j | j = 1, \ldots, N_p\}$, where N_p is the number of PSFs (instances) used in the simulation. Using the SMC method, a PSF instance is randomly selected from the set $\tilde{S}$ for each point exposed. Thus, the stochastic exposure distribution $e(x, y, z)$ in the resist for a feature is computed by

$$e(x,y,z) = \sum_x \sum_y d(x-x', y-y', 0) \cdot \mathrm{psf}_j(x', y', z), \qquad (1)$$

where $d(x, y, 0)$ is the dose distribution function defined on the surface of the resist and j is the index of the PSF instance

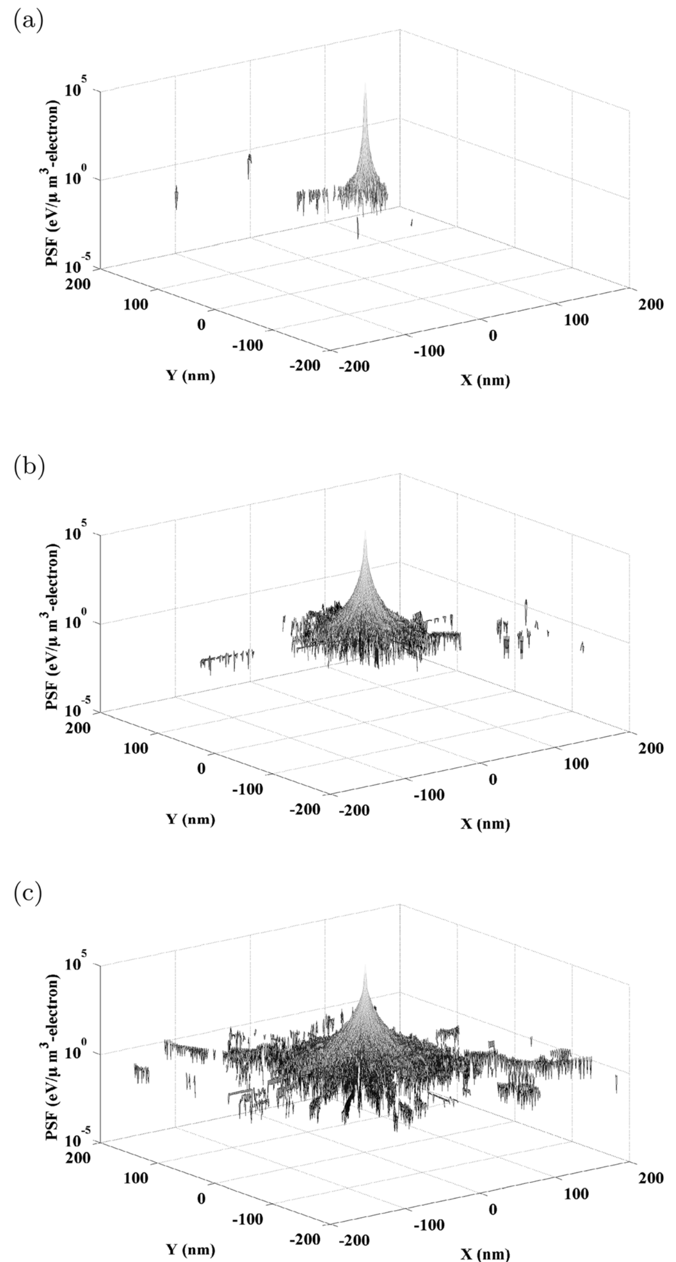

Fig. 1. Instance of stochastic PSF: (a) top, (b) middle, and (c) bottom layers of resist. PMMA on Si, dose: 640 μC/cm^2, resist thickness: 300 nm, beam energy: 50 keV, and beam diameter: 3 nm.

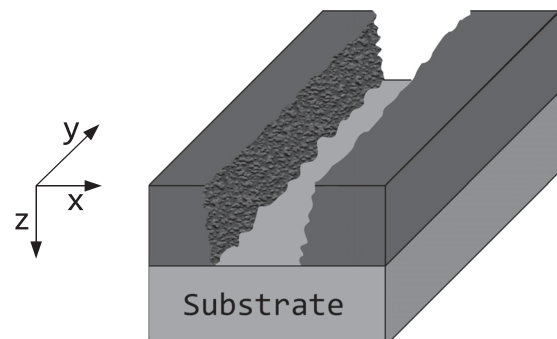

Fig. 2. 3D model of substrate system.

Redistribution subject to AVS license or copyright; see http://scitation.aip.org/termsconditions. Download to IP: 131.204.21.179 On: Tue, 11 Nov 2014 14:57:14

selected for the point $(x', y', 0)$. In the case of a uniform dose distribution, $d(x, y, 0)$ can be expressed as

$$d(x,y,0) = \begin{cases} D & \text{for exposed points} \\ 0 & \text{otherwise.} \end{cases} \tag{2}$$

B. Developing rate

For deriving the remaining resist profile from the exposure distribution in the resist, a resist development simulation may be employed. Since the exposure itself is not a quantitative measure of how fast the resist is developed, it needs to be converted to the developing rate.

1. Nonchemically amplified resist: PMMA

The exposure is converted to the developing rate through a nonlinear exposure-to-rate conversion formula, which reflects the characteristics of the developer and developing process. The conversion formula may be determined experimentally. In deriving the conversion formula, a long line with a width of 100 nm was exposed on the substrate system of 300 nm PMMA on Si with various dose levels. After the resist development (methyl isobutyl ketone:isopropanol = 1:2), the center depth is measured in the cross section of the remaining resist profile obtained for each dose level. Note that the resist is developed only vertically at the center of the line when the dose distribution within the line is uniform. The center depth is also obtained for each dose level through the simulation based on our 3D exposure model. By comparing the two sets of depth measurements obtained experimentally and via the simulation, the following mapping function has been derived:

$$r(x,y,z) = F[e(x,y,z)] = 3700 \cdot e^{-\left(\frac{e(x,y,z)-1.0\times10^{11}}{5.6\times10^{10}}\right)^2} - 80 \cdot e^{-\left(\frac{e(x,y,z)-9.0\times10^{9}}{9.0\times10^{9}}\right)^2} - 123, \tag{3}$$

where $r(x, y, z)$ is in nm/min and $e(x, y, z)$ is in eV/μm^3.

2. Chemically amplified resist: PHS

In the case of CAR, during the exposure process, PAG decompose and randomly create acid. The acid distribution $h(x,y,z)$ can be calculated by

$$h(x,y,z) = \mathrm{PAG}_0(x,y,z)(1 - e^{-C\cdot e(x,y,z)}), \tag{4}$$

where C is the exposure rate constant, and $\mathrm{PAG}_0(x, y, z)$ is the initial concentration of the PAG.[13]

A post-exposure bake (PEB) process is used to thermally induce a chemical reaction.[14] Some of polymer resins are initially blocked to inhibit the development process, which are referred to as the initial photoactive compound. These polymers can be deblocked by this chemical reaction, and the acid produced during the exposure process catalyzes the deblocking process making the resist development faster.

Assuming that the acid distribution $h(x, y, z)$ remains the same, the PEB process may be modeled by[13]

$$m(x,y,z) = e^{-k_{\mathrm{amp}} h(x,y,z)}, \tag{5}$$

where $m(x, y, z)$ represents the normalized concentration of unreacted blocking sites and k_{amp} is the acid amplification factor.

Then, the developing rate $r(x, y, z)$ at each point in the resist is calculated from its corresponding normalized concentration of unreacted blocking sites $m(x, y, z)$ using the Mack's dissolution model[15]

$$r(x,y,z) = (R_{\max} - R_{\min}) \frac{(a+1)\left(1-m(x,y,z)\right)^n}{a + \left(1-m(x,y,z)\right)^n} + R_{\min}, \tag{6}$$

$$a = \frac{n+1}{n-1}(1-m_{\mathrm{th}})^n, \tag{7}$$

where, $R_{\max}$, $R_{\min}$, and n are the maximum developing rate, the minimum developing rate, and the developer contrast, respectively, and m_{th} is a threshold of $m(x, y, z)$ corresponding to the inflection point of the developing rate curve.

C. Resist development

A common drawback of the conventional resist development simulation methods such as the cell removal method[16] is that they are computationally intensive. Therefore, it is not practical to employ them in an extensive simulation study. This time-consuming nature is mainly due to the incremental updating of cell states through a large number of iterations. In order to overcome the drawback, a new fast method for the resist development simulation was developed.[17] The method takes a path-based approach, i.e., the resist development process is modeled by development paths starting from the resist surface toward the boundaries of the (remaining) resist profile. Each path consists of a vertical path segment (representing vertical development) and lateral path segments (representing lateral development). All possible paths are traced without iterations, and those paths reaching the farthest points, given a developing time, determine the boundaries of the resist profile. It has been shown that this path-based method generates resist profiles well matched with those by the cell removal and fast marching methods and greatly reduces the simulation time, especially for features of regular shapes such as lines, rectangles, circles, etc.

Based on the developing rate distribution and a specified developing time, the resist development along each path can be determined and the 3D profile of remaining resist of a feature or pattern can be obtained.

D. Evaluation of LER

From the 3D profile of the remaining resist, the feature boundaries, i.e., edges, at each layer of resist can be obtained. Referring to Fig. 3, let $x_e(y)$ denote the actual edge location along one side of a feature (e.g., a long line) at a layer of resist. Note that Z is fixed at a layer of resist and therefore not included in $x_e(y)$. In this study, the LER at each layer of resist is quantified individually as three times the

Redistribution subject to AVS license or copyright; see http://scitation.aip.org/termsconditions. Download to IP: 131.204.21.179 On: Tue, 11 Nov 2014 14:57:14

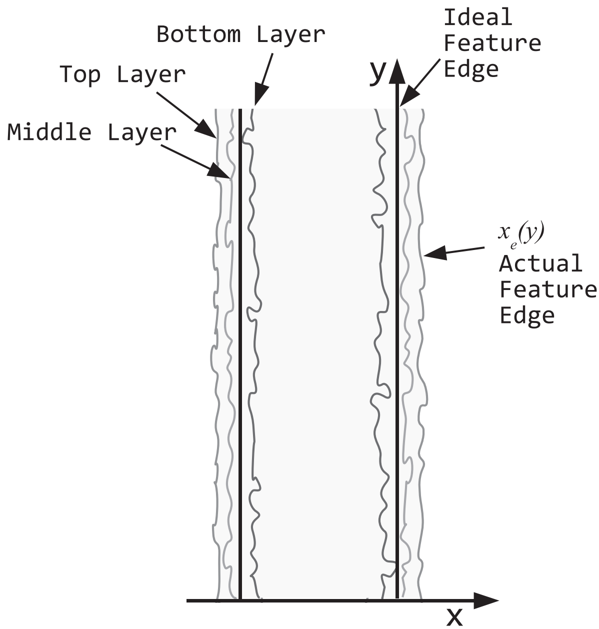

FIG. 3. LER at each layer is quantified individually as three times the standard deviation of edge location, i.e., 3σ-LER, along the length dimension of the feature.

standard deviation of edge location, i.e., 3σ-LER, along the length dimension of the feature. Then, the LER at that layer may be expressed as follows:

$$\mathrm{LER} = 3\sqrt{\frac{1}{N}\int (x_e(y) - \bar{x}_e(y))^2 dy}, \quad (8)$$

where $\bar{x}_e(y) = 1/N \int x_e(y)dy$ and N is the length of feature segment over which the LER is evaluated.

The LER at other layers of resist can be computed similarly with $x_e(y)$ for the corresponding layer.

E. Exposing interval

When a Gaussian beam is used in an e-beam system, i.e., the resist is exposed point-by-point, the exposing interval, i.e., the distance between adjacent points exposed by the beam, has two different effects. It affects the periodic variation of (spatial) exposure distribution and the number of electrons per shot (point). A smaller exposing interval reduces the periodic variation of exposure, which tends to make the LER smaller, but increases the randomness of PSF [because of a smaller number of electrons per shot leading to a lower signal-to-noise ratio (SNR)], which would increase the LER. That is, the exposing interval has two opposite effects on the LER. In Fig. 4, a simulation result on the effect of the exposing interval on the LER is provided. It shows that a smaller exposing interval leads to a smaller LER. This suggests that the reduced periodic variation of exposure by a smaller exposing interval tends to have a larger effect on the LER than the increased randomness of PSF. Therefore, in this study which focuses on minimization of the LER, the exposing interval is set to 1 nm in the simulation.

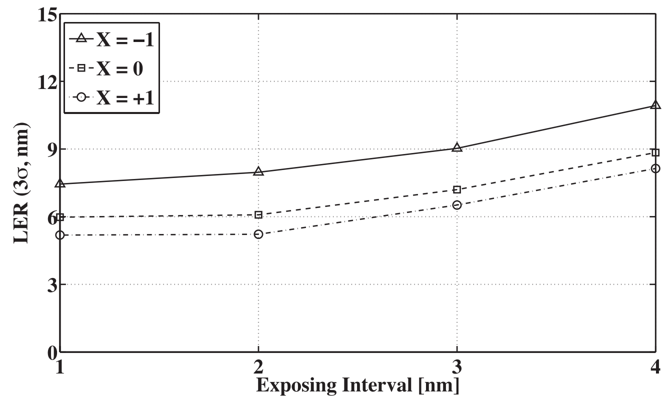

FIG. 4. Exposing interval dependency of the LER on different edge locations (PHS). Resist thickness: 300 nm, beam energy: 50 keV, beam diameter: 3 nm, dose: 32 μC/cm^2, bottom layer.

III. MINIMIZATION OF LER AND CD ERROR

In this section, two methods of minimizing the LER with the CD error taken into account are described. In one method, the feature dimensions are controlled with a uniform dose, to be referred to as shape control. In the other method, the dose is spatially controlled in addition to the shape control, to be referred to as shape and dose control.

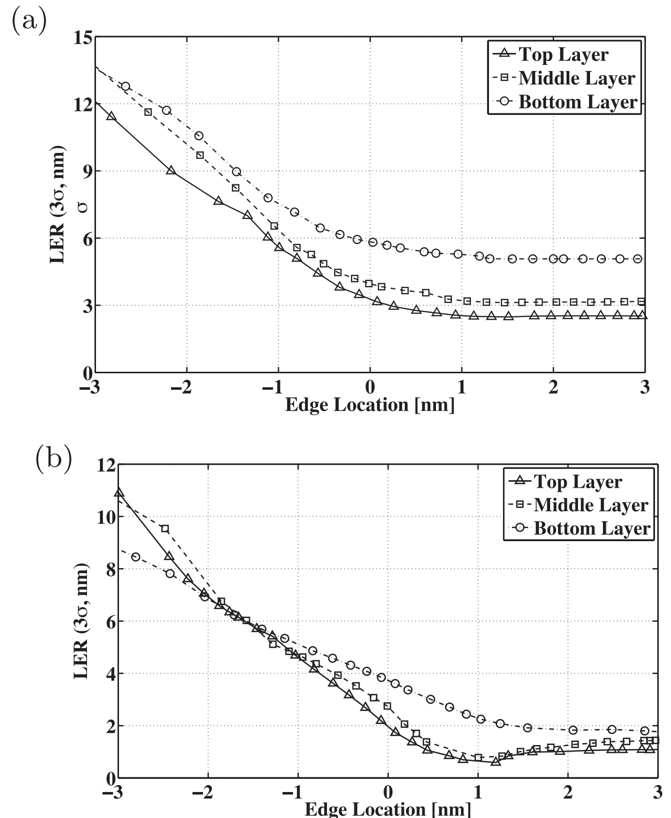

FIG. 5. Layer dependency of the LER on (a) PHS and (b) PMMA. For PHS, dose: 32 μC/cm^2, resist thickness: 300 nm, beam energy: 50 keV, beam diameter: 3 nm, and exposing interval: 1 nm. For PMMA, dose: 640 μC/cm^2, resist thickness: 300 nm, beam energy: 50 keV, beam diameter: 3 nm, and exposing interval: 1 nm.

Redistribution subject to AVS license or copyright; see http://scitation.aip.org/termsconditions. Download to IP: 131.204.21.179 On: Tue, 11 Nov 2014 14:57:14

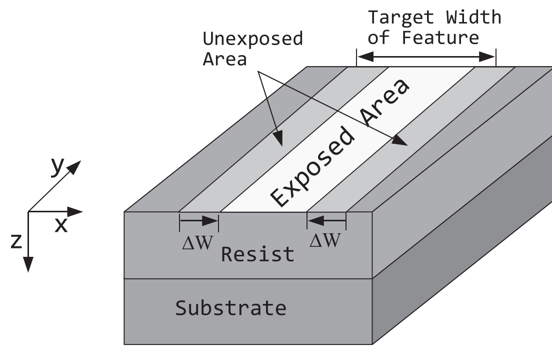

FIG. 6. In the shape control, the feature area to be exposed is shrunk from the feature boundary inward.

A. Shape control

In our previous work, the dependency of LER on different lithographic parameters has been investigated. As shown in Fig. 5, the LER is examined with the (actual) edge location varied from the inside ($X<0$) of a feature to the outside ($X>0$) by controlling the developing time. It is observed that the LER is high inside a feature, rapidly decreases over the feature edge, and then mostly stays low or slightly increases outside the feature. This is mainly due to the fact that the exposure (energy deposited in the resist) level quickly drops down from the exposed area (inside the feature) to the unexposed area (outside the feature) and the absolute stochastic fluctuation of exposure is smaller outside the feature, i.e., in the unexposed area. This behavior indicates that it might be possible to reduce the LER by shrinking the area of a feature to be exposed, from the feature boundary inward. This observation leads to the shape control method, which reduces the area to be exposed by ΔW on each side of the feature, instead of exposing the whole feature, as illustrated in Fig. 6. It needs to be pointed out that though this method is designed exploiting the behavior of LER mentioned above, the same idea of shrinking the feature area with or without explicit control of the dose level was effectively utilized in some of the PEC methods developed in the past such as the "undersize-overdose" method[18] and the shape correction.[19]

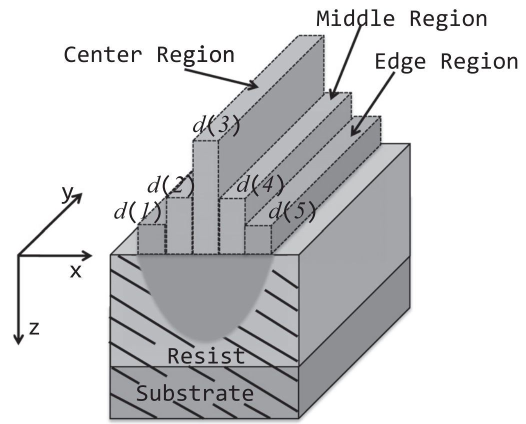

FIG. 7. Region-wise feature partitioning, where $d(i)$ is the dose to be given to region i. The total dose defined in this study is $\sum_{i=1}^{5} d(i)$.

Given a substrate system and a developing time, the initial total dose D_0 is set to be the minimum total dose required for exposing the whole feature (i.e., $\Delta W=0$) such that the CD error is minimized (total dose is defined as the integration of area dose over the feature width: see Fig. 7 where $d(i)=d(j)$ for all i, j in the case of a uniform dose). It is determined through a simple enumeration. In each step with a different total dose, the resist development simulation is employed and the CD error is evaluated from the remaining resist profile. The process is repeated with a number of total dose levels and the minimum total dose is determined to be the lowest total dose resulting in the smallest CD error. Then, the optimal amount of shrinking and the total dose are determined by an iterative method. In each iteration, ΔW is increased by a small amount and the feature area to be

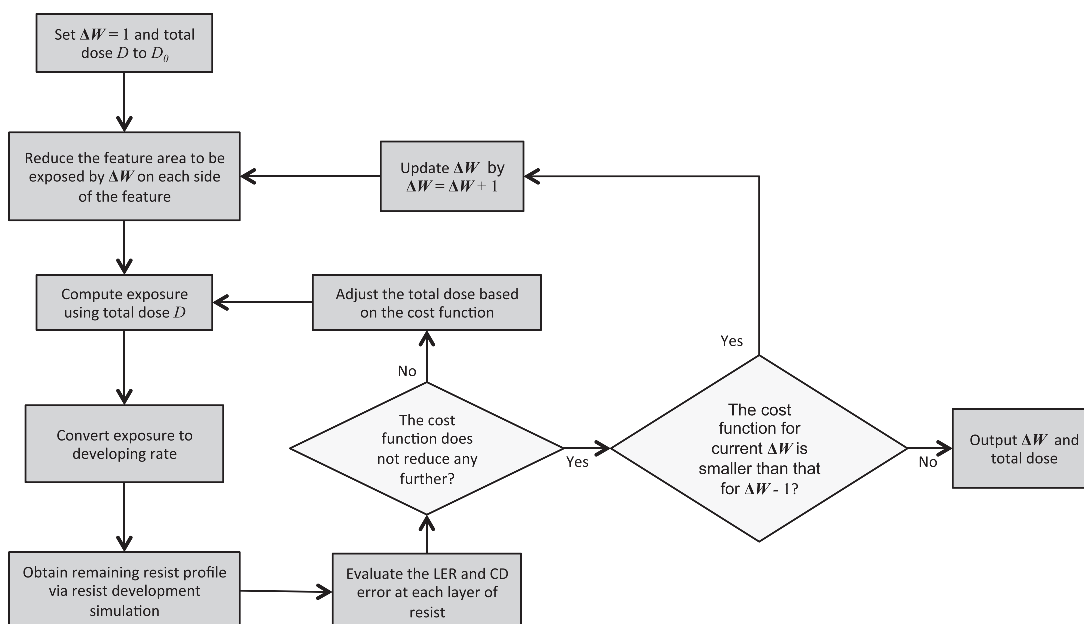

FIG. 8. Flowchart of the shape control method.

Redistribution subject to AVS license or copyright; see http://scitation.aip.org/termsconditions. Download to IP: 131.204.21.179 On: Tue, 11 Nov 2014 14:57:14

exposed is reduced by ΔW on each side of the feature. Then, the total dose D is adjusted so that the cost function is minimized. The iteration continues until the cost function does not reduce any further.

It may not be always possible to reduce both the LER and the CD error in each step of the optimization. To make the optimization procedure sufficiently general, a cost function involving the LER and the CD error may be employed. There can be many different ways to formulate the cost function. In our study, the following cost function is adopted:

$$\max\{\max_i\{\mathrm{LER}(i)\}, \max_i\{\mathrm{CD}_{\mathrm{error}}(i)\}\}, \tag{9}$$

where LER(i) and $\mathrm{CD}_{\mathrm{error}}(i)$ are the LER and width error at the i-th layer of resist.

The shape control method determines the ΔW and total dose to be used, given a developing time. Its complete procedure is depicted below assuming that the spatial resolution is limited to 1 nm (also refer to the flowchart in Fig. 8):

(1) Step 1: Set ΔW to 1 nm and D to D_0.
(2) Step 2: Reduce the feature area to be exposed by ΔW on each side of the feature.
(3) Step 3: Compute the exposure distribution using the total dose D.
(4) Step 4: Convert the exposure to the developing rate.
(5) Step 5: Obtain the remaining resist profile using a resist development simulation.
(6) Step 6: Evaluate the LER and feature width at the top, middle, and bottom layers of resist from the resist profile, and find the maximum LER and the maximum CD error among the layers.

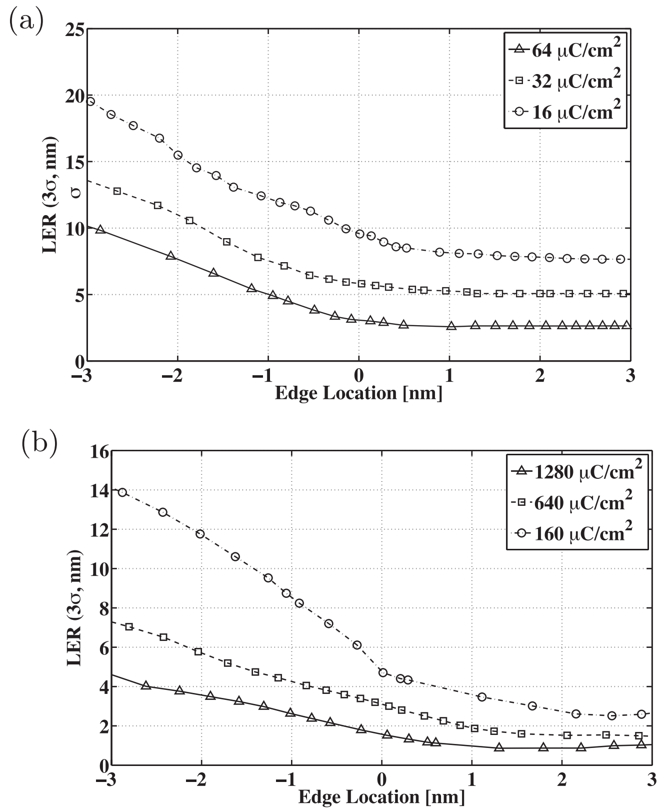

Fig. 9. Dose dependency of the LER on (a) PHS and (b) PMMA. For PHS, resist thickness: 300 nm, beam energy: 50 keV, beam diameter: 3 nm, exposing interval: 1 nm, bottom layer. For PMMA, resist thickness: 300 nm, beam energy: 50 keV, beam diameter: 3 nm, exposing interval: 1 nm, bottom layer.

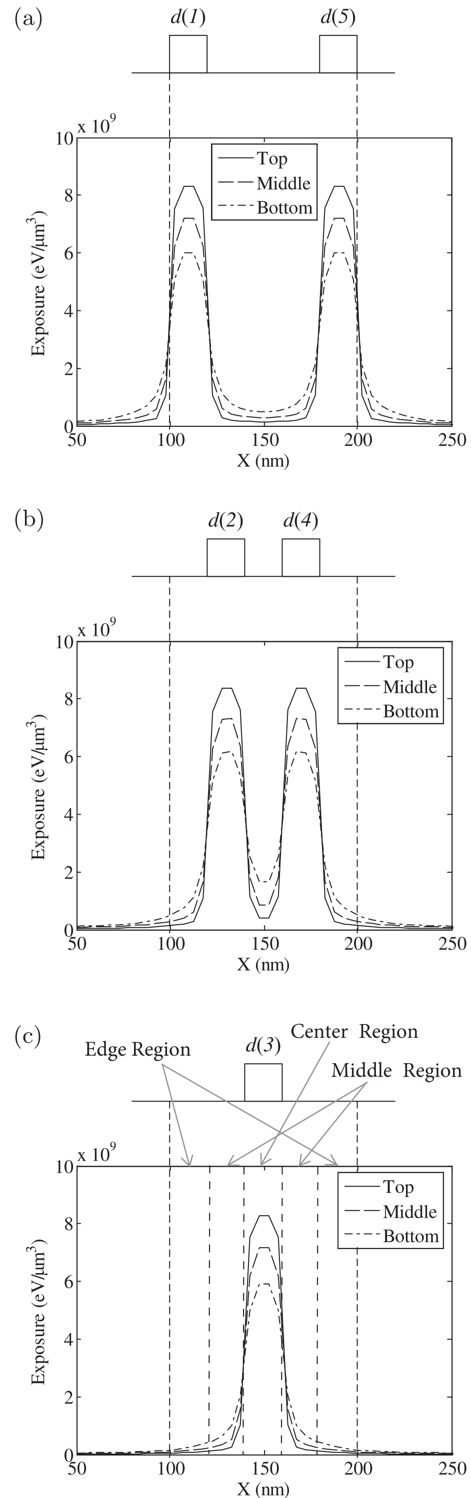

Fig. 10. Exposure distribution at the top, middle and bottom layers of resist when only the (a) edge regions, (b) middle regions, or (c) center region is exposed. Each figure shows the exposure contribution from the respective region to different layers and locations. In the figures, $d(1)$ and $d(5)$ are the doses given to two edge regions, $d(2)$ and $d(4)$ are the doses given to two middle regions, and $d(3)$ is the dose given to the center region.

Redistribution subject to AVS license or copyright; see http://scitation.aip.org/termsconditions. Download to IP: 131.204.21.179 On: Tue, 11 Nov 2014 14:57:14

(7) Step 7: If the cost function does not reduce any further, go to step 8. Otherwise, adjust the total dose based on the cost function and then go to step 3.
(8) Step 8: If the cost function for the current ΔW is smaller than that for $\Delta W - 1$ and the difference is larger than a certain threshold, update ΔW by $\Delta W = \Delta W + 1$, then go to step 2. Otherwise, go to step 9.
(9) Step 9: Output ΔW and total dose D.

While the shape control can reduce the LER, it has a few potential problems. Shrinking the area to be exposed makes the exposure contrast over the feature edge lower. The fluctuation and contrast of the exposure (equivalently developing rate) are the two main factors affecting the LER. A lower exposure contrast tends to lead to a larger LER. That is, the shrinking may not always reduce the LER. Also, the optimal amount of shrinking for minimizing the LER may not be optimal for minimizing the CD error in general. Moreover, the shrinking tends to increase the uncertainty of the edge location (due to the decreased exposure contrast over the edge). In order to avoid these potential problems and further reduce the LER and the CD error, controlling the dose spatially may be considered.

B. Shape and dose control

According to the previous study results, the LER decreases as the dose increases (for PHS: from 16 to 64 μC/cm^2 and for PMMA: from 160 to 1280 μC/cm^2, refer to Fig. 9). With a higher dose, there are more electrons per shot and therefore the exposure is averaged over more electrons leading to a better statistics, i.e., a smaller fluctuation of exposure and accordingly a smaller LER. Also, the SNR of the electron influx is given by

$$\mathrm{SNR} = \frac{N_0}{\sqrt{N_0}} = \sqrt{N_0}, \tag{10}$$

where N_0 denotes the number of electrons given to each exposed point.

From Eq. (10), it is easily understood that a higher dose also helps to enhance the SNR of electron influx and therefore reducing the fluctuation of exposure leading to a lower LER. These observations suggest that a further reduction of the LER may be achieved by controlling the spatial distribution of dose within a feature (in addition to the shape control). Note that this spatial dose control is a commonly used technique also in the proximity effect correction, i.e., reducing the CD error. Therefore, the spatial distribution of dose is controlled for minimizing the LER and the CD error. In order to avoid a high complexity of the optimization procedure and also have sufficient spatial control of the dose distribution, the area (to be exposed) of a line feature is partitioned into five regions along its length dimension (refer to Fig. 7) and the dose of each region is to be determined.

The dose given to a different part of the feature has a different effect on the level and stochastic fluctuation of the exposure at a different layer and location in the resist (refer to Fig. 10). For example, as shown in Fig. 10(a), the exposure contributions from the edge regions to the respective edge regions decrease from the top layer to the bottom layer. On the other hand, the exposure contributions from the middle [see Fig. 10(b)] or center region [see Fig. 10(c)] to the edge regions increase from the top layer to the bottom layer. Hence, in order to reduce the LER or CD error at a certain layer, it would be more effective to control the dose of the region, which affects the layer relatively more (than those of other regions).

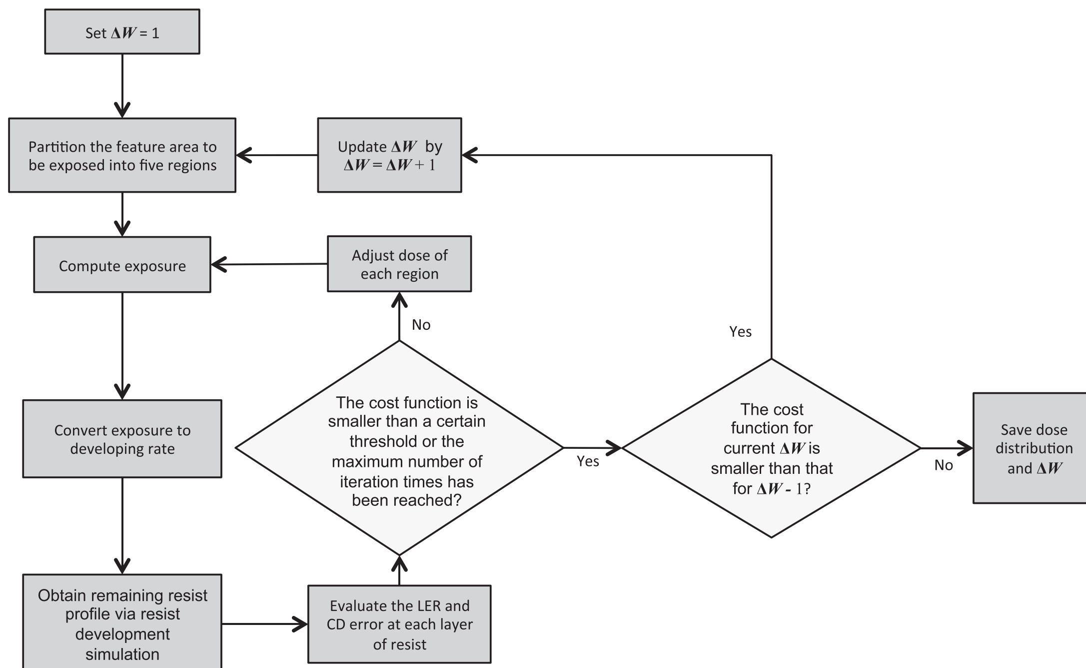

Fig. 11. Flowchart of the shape and dose control method.

Redistribution subject to AVS license or copyright; see http://scitation.aip.org/termsconditions. Download to IP: 131.204.21.179 On: Tue, 11 Nov 2014 14:57:14

For example, assume that the current dose distribution yields an overcut profile and the largest LER at the bottom layer. To reduce the LER at the bottom layer, the exposure level at the bottom layer needs to be increased. To reduce the width at the top layer and increase the width at the bottom layer (to achieve a vertical sidewall), the exposure level at the top layer needs to be reduced while the exposure level at the bottom layer needs to be increased.

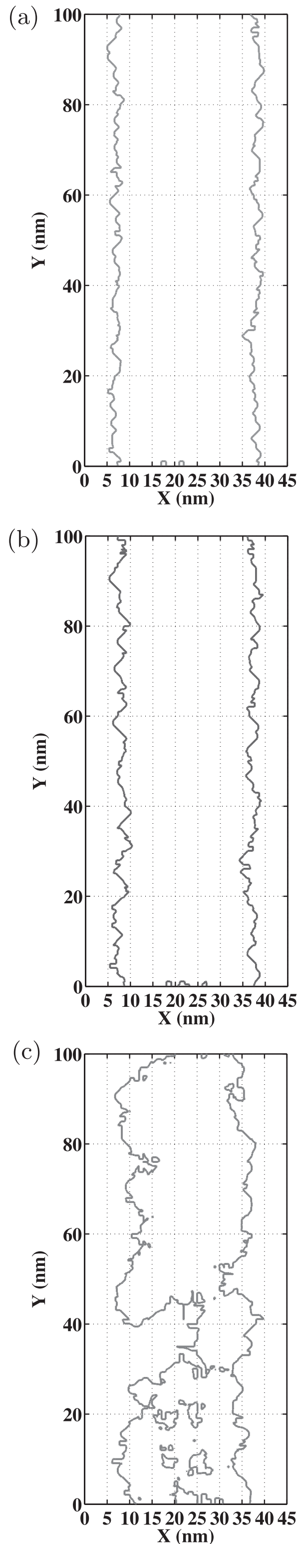

FIG. 12. Contour of remaining resist profile at (a) top, (b) middle, and (c) bottom layers without shape control ($\Delta W = 0$ nm). PHS on Si, total dose: 7.59×10^{-5} μC/cm, resist thickness: 300 nm, beam energy: 50 keV, beam diameter: 3 nm, and exposing interval: 1 nm, feature size: 25 nm.

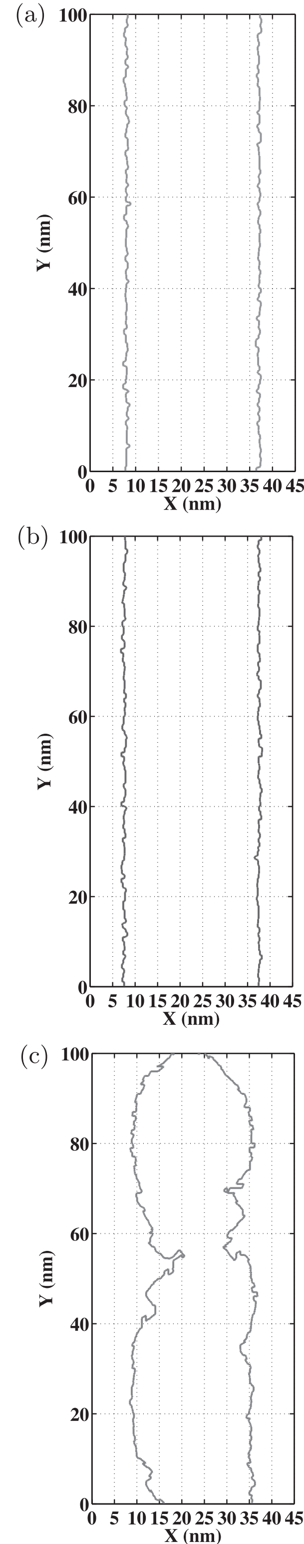

FIG. 13. Contour of remaining resist profile at (a) top, (b) middle, and (c) bottom layers without shape control ($\Delta W = 0$ nm). PMMA on Si, total dose: 109.60×10^{-5} μC/cm, resist thickness: 300 nm, beam energy: 50 keV, beam diameter: 3 nm, and exposing interval: 1 nm, feature size: 25 nm.

Redistribution subject to AVS license or copyright; see http://scitation.aip.org/termsconditions. Download to IP: 131.204.21.179 On: Tue, 11 Nov 2014 14:57:14

Therefore, in order to reduce the LER at the bottom layer and make the sidewall more vertical, one may increase the dose of the center region and reduce the dose of the edge region. The reduced dose in the edge region makes the developing rate in the edge region at the top layer decrease and therefore the feature width at the top layer narrower. Meanwhile, the increased dose in the center region makes the developing rate of vertical development in the center

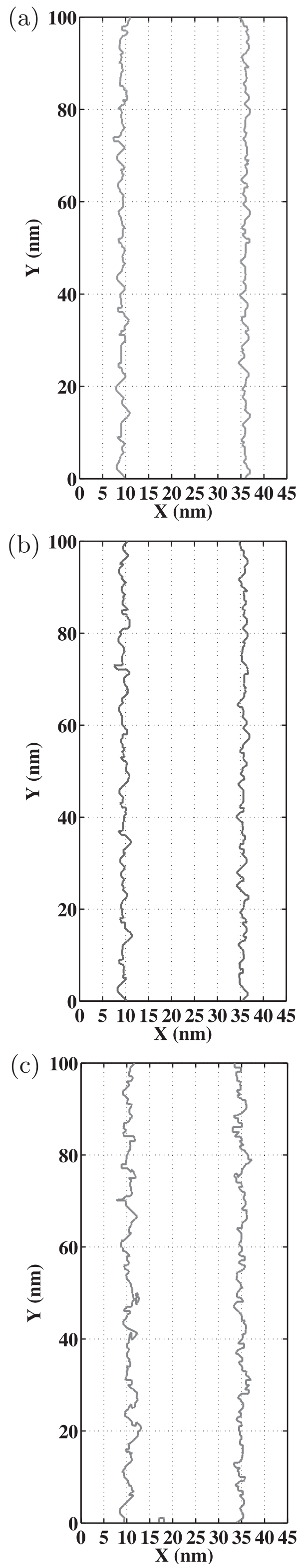

FIG. 14. Contour of remaining resist profile at (a) top, (b) middle, and (c) bottom layers with shape control ($\Delta W = 3$ nm). PHS on Si, total dose: 11.04×10^{-5} μC/cm, resist thickness: 300 nm, beam energy: 50 keV, beam diameter: 3 nm, and exposing interval: 1 nm, feature size: 25 nm.

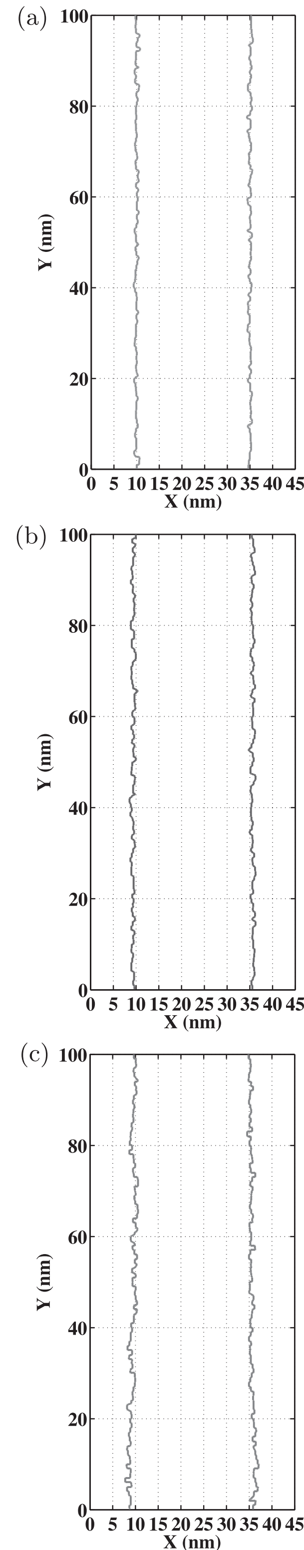

FIG. 15. Contour of remaining resist profile at (a) top, (b) middle, and (c) bottom layers with shape control ($\Delta W = 3$ nm). PMMA on Si, total dose: 117.37×10^{-5} μC/cm, resist thickness: 300 nm, beam energy: 50 keV, beam diameter: 3 nm, and exposing interval: 1 nm, feature size: 25 nm.

Redistribution subject to AVS license or copyright; see http://scitation.aip.org/termsconditions. Download to IP: 131.204.21.179 On: Tue, 11 Nov 2014 14:57:14

region higher and therefore allows more time for lateral development at the bottom layer (to catch up with the top layer). Also, it helps to increase the exposure level at the bottom layer relative to the upper layers. Therefore, at the bottom layer, the feature width increases and the LER decreases (the exposure fluctuation is reduced due to the increased exposure level).

The shape and dose control method starts with determining how much a feature area to be exposed is to be shrunk, i.e., shape control. Since a sophisticated procedure for optimizing the spatial distribution of dose is employed later, the minimum, instead of optimal, amount of shrinking is determined in this step. This also helps to prevent the exposure contrast over the edge from decreasing too much, to avoid the potential problems of the shape control method (refer to Sec. III A). Then, the feature area is partitioned into five regions along the length dimension of the feature for controlling the dose spatially. The dose of each region is derived through an iterative procedure. In each iteration, the LER and the CD error at each layer of the resist are computed through the simulation of resist development, and the dose of each region is adjusted, considering its effect on the exposure distribution (level and stochastic fluctuation), such that the cost function in Eq. (9) is reduced.

The shape and dose control method determines the ΔW and spatial dose distribution to be used, given a developing time. The total dose is set in the same way as the initial total dose is determined in the shape control method and remains fixed. The complete procedure is depicted below (also refer to the flowchart in Fig. 11):

(1) Step 1: Set ΔW to 1 nm.
(2) Step 2: Partition the feature area to be exposed into five regions.
(3) Step 3: Calculate the exposure distribution in the resist based on the current spatial dose distribution (start with a uniform dose distribution).
(4) Step 4: Convert the exposure distribution to the developing rate.
(5) Step 5: Derive the remaining resist profile by employing a simulation of the resist development process.
(6) Step 6: Evaluate the LER and the CD error at each layer of the resist from the resist profile.
(7) Step 7: If the cost function is smaller than a certain threshold or the maximum number of iterations has been reached, go to step 8. Otherwise, adjust the dose of each region based on the cost function and then go to step 3.
(8) Step 8: If the cost function for the current ΔW is smaller than that for $\Delta W - 1$ and the difference is larger than a certain threshold, update ΔW by $\Delta W = \Delta W + 1$, then go to step 2. Otherwise, go to step 9.
(9) Step 9: Save ΔW and the current spatial dose distribution.

IV. RESULTS AND DISCUSSION

The effectiveness of the proposed methods for minimization of the LER and the CD error has been analyzed through an extensive simulation. The CASINO software is employed to generate stochastic PSFs assuming a Gaussian-shaped electron beam. Two substrate systems are employed in this study, PMMA on Si, and PHS on Si. The resist is partitioned into five layers in the simulation, and the top, middle, and bottom layers are considered in the analysis. The 3D exposure distribution in the resist for a single line feature of size $25 \times 120\,\mathrm{nm}^2$ is computed layer-by-layer within a window of size $65 \times 100\,\mathrm{nm}^2$. Through the resist development simulation, the remaining resist profile is obtained on each layer and the LER and the CD error are evaluated. In order to avoid a biased result, the simulation is repeated five times in each case.

The default values of the simulation parameters are as follows. For PMMA, the resist thickness is 300 nm, the beam energy is 50 keV, the beam diameter is 3 nm, and the exposing interval is 1 nm. For PHS, the resist thickness is 300 nm, the beam energy is 50 keV, the beam diameter is 3 nm, the exposing interval is 1 nm, C is 0.024741, the average initial PAG density is 0.05 nm^3, k_{amp} is 0.22 1/s, m_{th} is 0.61, n is 6, $R_{\max}$ is 55 nm/s, and $R_{\min}$ is 0.15 nm/s. Unless specified otherwise, these default values are used in the simulation.

A. Shape control

The contours (feature boundaries) of resist profiles obtained when the whole feature is exposed without any shape control are provided in Figs. 12 and 13 and those obtained by the shape control method in Figs. 14 and 15. In the results for both types of resists with no shape control, it is seen that the LER is significantly larger at a lower layer and the CD error is substantial at upper layers. Also, the bottom layer is not fully developed, especially in the case of CAR (PHS), leading to a large CD error. However, significant improvement is clearly visible when the shape control is applied. The LER is reduced at all layers and better balanced

TABLE I. Maximum LER and maximum CD error for different ΔW. PHS on Si, resist thickness: 300 nm, beam energy: 50 keV, beam diameter: 3 nm, exposing interval: 1 nm, and feature size: 25 nm.

	No shape control	ΔW (nm)				
	$\Delta W = 0$	1	2	3	4	5
CD error (nm)	6.053	4.015	2.719	1.703	2.289	5.326
LER (3σ, nm)	18.623	8.963	6.636	4.920	5.946	8.006
Total dose ($10^{-5}\,\mu$C/cm)	7.59	8.32	9.49	11.04	23.18	36.43

TABLE II. Maximum LER and maximum CD error for different ΔW. PMMA on Si, resist thickness: 300 nm, beam energy: 50 keV, beam diameter: 3 nm, exposing interval: 1 nm, and feature size: 25 nm.

	No shape control	ΔW (nm)				
	$\Delta W = 0$	1	2	3	4	5
CD error (nm)	4.868	2.824	1.203	1.377	2.791	7.449
LER (3σ, nm)	12.914	5.917	3.373	2.997	3.655	8.032
Total dose ($10^{-5}\,\mu$C/cm)	109.60	110.39	114.08	117.37	126.69	141.74

Redistribution subject to AVS license or copyright; see http://scitation.aip.org/termsconditions. Download to IP: 131.204.21.179 On: Tue, 11 Nov 2014 14:57:14

among layers. Also, the average feature width is very close to the target width at all layers, i.e., very small CD errors. As expected, the LER for PHS is substantially larger than that for PMMA before and after the minimization.

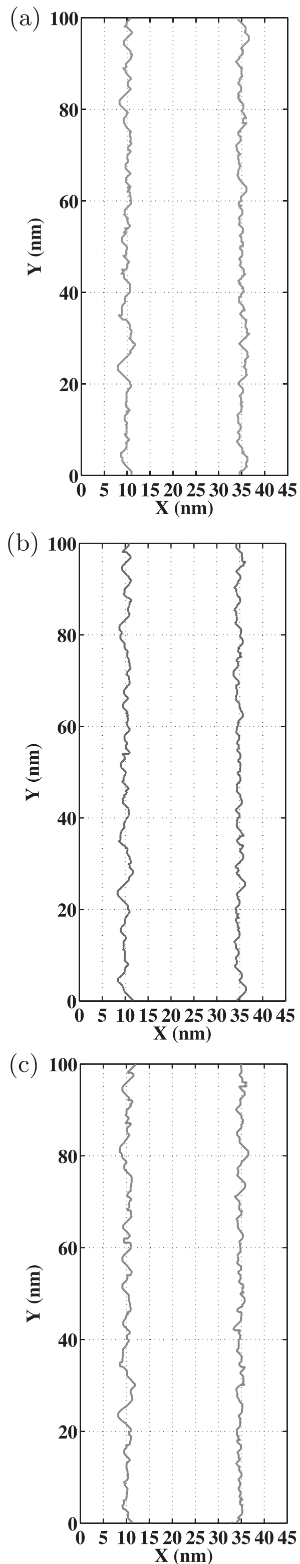

FIG. 16. Contour of remaining resist profile at (a) top, (b) middle, and (c) bottom layers with shape and dose control ($\Delta W = 2$ nm). PHS on Si, total dose: 7.59×10^{-5} μC/cm, resist thickness: 300 nm, beam energy: 50 keV, beam diameter: 3 nm, and exposing interval: 1 nm, feature size: 25 nm.

A quantitative comparison between without and with the shape control is made for each resist type using the maximum LER and maximum CD error (among layers). Also, the total dose required is considered. The results for PHS are in

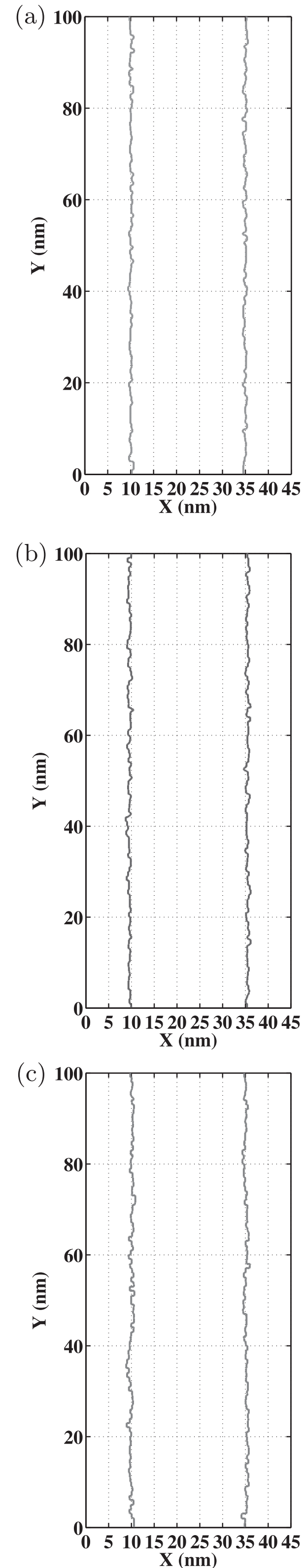

FIG. 17. Contour of remaining resist profile at (a) top, (b) middle, and (c) bottom layers with shape and dose control ($\Delta W = 2$ nm). PMMA on Si, total dose: 109.60×10^{-5} μC/cm, resist thickness: 300 nm, beam energy: 50 keV, beam diameter: 3 nm, and exposing interval: 1 nm, feature size: 25 nm.

Redistribution subject to AVS license or copyright; see http://scitation.aip.org/termsconditions. Download to IP: 131.204.21.179 On: Tue, 11 Nov 2014 14:57:14

TABLE III. LER, CD error, total dose, and ΔW for shape control.

			Shape control, uniform dose							
			CD error (nm)			LER (3σ, nm)				
Resist type	Resist thickness (nm)	Beam energy (keV)	Top layer	Middle layer	Bottom layer	Top layer	Middle layer	Bottom layer	Total dose 10^{-5} μC/cm	ΔW (nm)
CAR	100	50	2.230	1.469	0.200	4.396	5.181	6.754	13.20	3
CAR	100	25	0.413	0.169	0.155	2.791	2.962	3.241	9.14	4
CAR	300	50	1.703	0.987	0.585	3.285	3.682	4.920	11.04	3
PMMA	100	25	0.108	0.421	0.202	1.765	2.167	3.151	98.03	2
PMMA	300	50	0.347	0.377	1.377	1.778	1.956	2.997	117.37	3
PMMA	500	50	0.302	3.275	1.427	1.966	2.213	4.663	195.63	5

Table I and those for PMMA in Table II. The results show that the LER drops quickly with ΔW increasing. However, as ΔW increases beyond 3 nm, the LER begins to increase. This may be due to the fact that the exposure contrast over the edge becomes lower and the relative exposure fluctuation at the edge becomes larger with the increase of ΔW. Also, the total dose keeps increasing with ΔW increasing. For a larger ΔW, the edge region is farther away from the exposed area and therefore an increasingly higher dose (growing faster than linear with ΔW) is required for full development of the resist. In addition, the optimal ΔW for the LER is not necessarily the same as that for the CD error as can be seen in Table II. ΔW needs to be 3 nm to minimize the LER while it should be 2 nm to minimize the CD error.

B. Shape and dose control

The contours of the resist profiles obtained by the shape and dose control method are provided in Figs. 16 and 17. They are noticeably smoother compared to the results by the shape control method (in Figs. 14 and 15). The largest improvement can be seen at the bottom layers, especially in the case of CAR.

In Tables III and IV, the shape control method and the shape and dose control method are compared in terms of the LER, CD error, and total dose. From the tables, it can be seen that, compared to the shape control method, the shape and dose control method achieves significantly smaller LER and the CD error at all layers in most cases while requiring a lower total dose. The shape and dose control method reduces both of the maximum LER and the maximum CD error in all cases. That is, the resist profiles by the shape and dose control method are more balanced in the LER and the CD error among layers. Also, the largest reduction of the LER is achieved at the bottom layer in most cases. In addition, ΔW is smaller for the shape and dose control method, which prevents the exposure contrast over the feature edge from decreasing too much.

Another observation that can be made in the tables is that ΔW is larger for a thicker resist or a lower beam energy, which indicates that a larger ΔW is required for a lower exposure contrast or a larger aspect ratio.

V. SUMMARY

For a pattern of nanoscale features, the LER can limit the minimum feature size and feature density that are achievable by e-beam lithography. In this study, a computational approach is taken in developing an effective method to minimize the LER, taking the CD error also into account. The LER and the CD error vary along the resist-depth dimension, and therefore, a 3D model is employed instead of a 2D model used in most of the previous work.

TABLE IV. LER, CD error, total dose, and ΔW for shape and dose control.

			Shape and dose control							
			CD error (nm)			LER (3σ, nm)				
Resist type	Resist thickness (nm)	Beam energy (keV)	Top layer	Middle layer	Bottom layer	Top layer	Middle layer	Bottom layer	Total dose 10^{-5} μC/cm	ΔW (nm)
CAR	100	50	0.012	0.402	0.487	2.042	2.362	2.960	10.52	2
CAR	100	25	0.065	0.047	0.058	2.427	2.576	3.051	5.60	3
CAR	300	50	0.581	0.122	0.946	3.661	3.752	3.847	7.59	2
PMMA	100	25	0.234	0.061	0.156	1.715	1.931	2.145	92.01	1
PMMA	300	50	0.243	0.861	0.069	1.530	1.623	2.261	109.60	2
PMMA	500	50	0.614	2.629	0.310	2.025	2.243	3.823	165.20	3

Redistribution subject to AVS license or copyright; see http://scitation.aip.org/termsconditions. Download to IP: 131.204.21.179 On: Tue, 11 Nov 2014 14:57:14

Through an extensive simulation, it has been shown that that the proposed methods can significantly reduce the LER and the CD error. The shape control method is simpler and computationally less expensive. However, it may not optimally balance between the LER and the CD error, and has a few potential problems mainly due to the decreased exposure contrast over the feature edge. On the other hand, the shape and dose control method is able to find a better balance between the LER and the CD error by utilizing both shape adjustment and spatial dose control without increasing the total dose. Also, it tends to limit the amount of shape adjustment and therefore avoids the problems of the shape control method. Therefore, when the spatial control of the dose is available on an e-beam system, the shape and dose control method is preferred. The effectiveness of the two methods has been verified through the simulation with two different types of resists.

It needs to be pointed out that a computer simulation may not capture perfectly or completely all the details of the processes involved in the e-beam exposure and resist development and therefore the LER and the CD errors obtained from the simulation can be different from the real values. However, it is hoped that the results reported in this paper show the trends in the behaviors of LER and the CD error with sufficient accuracy and can be referred to in future efforts to minimize the LER and the CD error.

ACKNOWLEDGMENT

This work was supported by a research grant from Samsung Electronics Co., Ltd.

[1]R. Murali, D. Brown, K. Martin, and J. Meindl, J. Vac. Sci. Technol., B **24**, 2936 (2006).
[2]F. Hu and S.-Y. Lee, J. Vac. Sci. Technol., B **21**, 2672 (2003).
[3]Q. Dai, S.-Y. Lee, S.-H. Lee, B.-G. Kim, and H.-K. Cho, J. Vac. Sci. Technol., B **29**, 06F314 (2011).
[4]Q. Dai, S.-Y. Lee, S.-H. Lee, B.-G. Kim, and H.-K. Cho, Microelectron. Eng. **88**, 902 (2011).
[5]A. Schleunitz and H. Schift, J. Micromech. Microeng. **20**, 095002 (2010).
[6]E. Seo, B. Kyung Choi, and O. Kim, Microelectron. Eng. **53**, 305 (2000).
[7]S.-Y. Lee and B. D. Cook, IEEE Trans. Semicond. Manuf. **11**, 108 (1998).
[8]G. Owen and P. Rissman, J. Appl. Phys. **54**, 3573 (1983).
[9]J. Bolten and T. Wahlbrink, Microelectron. Eng. **87**, 1041 (2010).
[10]J. Bolten and T. Wahlbrink, Microelectron. Eng. **88**, 1910 (2011).
[11]W. Cho and H. Kim, J. Korean Phys. Soc. **56**, 1767 (2010).
[12]X. Zhao, S.-Y. Lee, S.-H. Lee, B.-G. Kim, and H.-K. Cho, J. Vac. Sci. Technol., B **30**, 06F308 (2012).
[13]K. Suzuki, J. Shears, and B. Smith, *Microlithography: Science and Technology* (Marcel Dekker, New York, 1998).
[14]N. Jakatdar, X. Niu, and C. J. Spanos, Proc. SPIE **3332**, 578 (1998).
[15]C. A. Mack, J. Electrochemical Soc. **134**, 148(1987).
[16]Y. Hirai, S. Tomida, K. Ikeda, M. Sasago, M. Endo, S. Hayama, and N. Nomura, IEEE Trans. Comput. Aided Des. **10**, 802 (1991).
[17]Q. Dai, R. Guo, S.-Y. Lee, J. Choi, S.-H. Lee, I.-K. Shin, C.-U. Jeon, B.-G. Kim, and H.-K. Cho, Microelectron. Eng. **127**, 86 (2014).
[18]V. A. Guzenko and B. Pedrini, Microelectron. Eng. **121**, 127 (2013).
[19]B. D. Cook and S.-Y. Lee, IEEE Trans. Semicond. Manuf. **11**, 117 (1998).

Redistribution subject to AVS license or copyright; see http://scitation.aip.org/termsconditions. Download to IP: 131.204.21.179 On: Tue, 11 Nov 2014 14:57:14